Review Article

Ahmad Adlie Shamsuri*, Mohd Zuhri Mohamed Yusoff, Khalina Abdan, and Siti Nurul Ain Md. Jamil

Ionic liquid-modified carbon-based fillers and their polymer composites – A Raman spectroscopy analysis

https://doi.org/10.1515/rams-2024-0070 received June 04, 2024; accepted November 02, 2024

Abstract: In the field of advanced materials, carbon-based fillers are crucial for crafting high-performance polymer composites. Continual innovations in modifying these fillers are expanding the capabilities of polymer composite materials, heralding new advancements in diverse technological areas. Ionic liquids provide innovative methods for modifying carbon-based fillers to improve the performance of polymer composites. In this concise review, numerous carbon-based fillers used for modification, ionic liquids utilized in the modification, and polymer matrices employed in polymer composites are classified. In addition, the impact of ionic liquids on the interactional and structural properties of carbon-based fillers and their polymer composites, as analyzed via Raman spectroscopy, is concisely explained. This review provides a succinct analysis that deepens the understanding of the Raman spectroscopic results pertaining to various carbon-based fillers and polymer composites. In brief, Raman analyses indicate that carbon-based fillers modified with ionic liquids and their composites exhibit upshifted peak positions and higher intensity ratios compared to their unmodified fillers. The upshifts in peak positions are linked to interactions between the fillers and ionic liquids or between the modified fillers and polymer matrices. Higher intensity ratios in these modified fillers and polymer composites suggest increased structural defects in the fillers.

Mohd Zuhri Mohamed Yusoff, Khalina Abdan: Laboratory of Biocomposite Technology, Institute of Tropical Forestry and Forest Products, Universiti Putra Malaysia, 43400 UPM, Serdang, Selangor, Malaysia

Siti Nurul Ain Md. Jamil: Department of Chemistry, Faculty of Science, Universiti Putra Malaysia, 43400 UPM, Serdang, Selangor, Malaysia; Centre for Foundation Studies in Science of Universiti Putra Malaysia, Universiti Putra Malaysia, 43400 UPM, Serdang, Selangor, Malaysia

Keywords: ionic liquid, carbon-based filler, polymer composite, Raman spectroscopy, peak position, intensity ratio

1 Introduction

In the area of advanced materials, carbon-based fillers stand as essential components in the development of highperformance polymer composites. These fillers derived from various forms of carbon, such as carbon black, graphite, graphene, and carbon nanotubes [1], are renowned for their exceptional properties, which include high thermal conductivity, electrical conductivity, and mechanical strength [2]. Their incorporation in polymer matrices can significantly enhance the physical properties of the base material [3], leading to composites that are robust, lightweight, and capable of operating under a wide range of environmental conditions [4]. Carbon-based fillers substantially improve the thermomechanical properties of polymer-based composites due to their superior mechanical and thermal characteristics. When modified and incorporated into polymer matrices, these fillers contribute to advanced composite materials that offer enhanced strength, conductivity, and stability [5]. This versatility makes carbon-based fillers highly sought after in numerous industrial applications, ranging from electronic to aerospace engineering, where they contribute to electrical conductivity and material durability [6]. The morphology and surface chemistry of these fillers play crucial roles in their interactions with polymer matrices [7]. Modifications at the molecular level can tailor their dispersion and compatibility [3,8,9], influencing the overall performance characteristics of the composites. As research progresses, the modification of novel carbon-based fillers continues to push the boundaries of polymer composite material capabilities, promising new innovations across various technological fields. Moreover, the environmental aspects of their modification are becoming increasingly important considerations as industries strive for sustainability, emphasizing eco-friendly practices and resourceefficient methodologies in manufacturing processes.

^{*} Corresponding author: Ahmad Adlie Shamsuri, Laboratory of Biocomposite Technology, Institute of Tropical Forestry and Forest Products, Universiti Putra Malaysia, 43400 UPM, Serdang, Selangor, Malaysia, e-mail: adlie@upm.edu.my

2 — Ahmad Adlie Shamsuri et al. DE GRUYTER

Ionic liquids, characterized by their unique properties, such as low volatility, thermal stability, and tunable solubility [10-12], offer innovative ways to modify carbonbased fillers to enhance polymer composites' performance [9]. When used as modifying agents, ionic liquids can impart specific functionalities to the surfaces of carbonbased fillers such as graphene, graphene oxide, and carbon nanotubes [13–15]. These functionalities can lead to improved dispersion within polymer matrices [16,17], enhanced interfacial bonding [18], and increased electrical and thermal conductivities [13]. The modification mechanism involves the interaction between the ionic liquid and the carbon filler. often resulting in a tailored surface chemistry that is better suited for specific applications. For instance, the introduction of ionic liquids can reduce the agglomeration of nanofillers and promote a more homogeneous distribution throughout the polymer matrix [19,20], which is crucial for achieving the desired mechanical, thermal, and electrical properties in the final composites. Moreover, the use of ionic liquids in surface modification is aligned with green chemistry principles, offering a less toxic and environmentally benign alternative to conventional organic solvents and chemical treatments [7,21]. This approach not only extends the functional range of traditional carbon-based fillers but also opens new possibilities for the design of next-generation materials that meet stringent performance and environmental criteria.

Raman spectroscopy is highly effective for characterizing carbon materials, as it offers insights into various characteristics, including electronic structure, photonic structure, and defect structure [15]. It emerges as an essential analytical technique in the study of ionic liquid-modified carbon-based fillers [22]. This non-destructive spectroscopic method is particularly valuable for probing the molecular structure and bonding environment of modified fillers [23,24]. By delivering detailed comprehensions into the chemical interactions at the molecular level and structural characteristics [3,25], Raman spectroscopy helps elucidate how ionic liquids change the properties of carbon-based fillers. The unique Raman spectra obtained through Raman analysis provide crucial data regarding

the functionalization of the filler surfaces [2]. For instance, shifts in peak positions or changes in intensity ratios can indicate the presence of ionic liquid molecules [18,26] or the degree of crystallinity of carbon fillers [27,28]. These spectroscopic signatures are vital for verifying the successful modification of the fillers and for understanding the dynamics of these modifications under various environmental conditions [29]. Moreover, Raman spectroscopy aids in assessing the efficacy and constancy of the modifications [22], which are critical factors in tuning filler properties. The technique's sensitivity to structural changes makes it an indispensable tool in the ongoing development and refinement of ionic liquid domains in polymer composite materials.

The application of Raman spectroscopy to analyze ionic liquid-modified carbon-based fillers within polymer composites offers profound insights into their interactions and structures [30]. This technique is crucial for confirming modified-filler loading [31], which is essential to support the changes in mechanical, thermal, and electrical properties of the composites [32], highlighting the significant value of Raman spectroscopy. This review aims to emphasize recent advancements in the utilization of ionic liquids for polymer composites, with a particular focus on comprehensions derived from Raman spectroscopic analyses. So far, there has been limited literature that specifically reviewed carbon-based fillers, ionic liquids, polymer matrices, and their analysis through Raman spectroscopy in ionic liquid-modified carbon-based fillers and their polymer composites. This concise review seeks to address this gap by exploring the way ionic liquids modify carbonbased fillers and polymer composites, especially in terms of their effects on Raman spectroscopy results. Through investigating the role of ionic liquids, this review provides a succinct overview of the interactions and structures within these materials. The goal is to deepen the understanding of how ionic liquids impact the interactional and structural properties of the fillers and their composites, as observed in Raman analyses, thereby enriching the overall knowledge base in materials science.

Table 1: Examples of carbon-based fillers used for modification with ionic liquids

Carbon-based filler	Abbreviation Ref.		
Carbon black	СВ	[16]	
Carboxylated multiwalled carbon nanotubes	MWCNT-COOH	[37]	
Graphene	Gra	[15,22,24,35,38,39]	
Graphene oxide	GO	[9,11,14,18,23,26,29,34,40-42]	
Multiwalled carbon nanotubes	MWCNTs	[2,3,6,7,13,17,20,25,27,28,30,31,33,43-49]	
Reduced graphene oxide	RGO	[19,50]	
Rice bran carbon	RBC	[51]	

2 Carbon-based fillers for modification with ionic liquids

Table 1 presents examples of carbon-based fillers used for modification with ionic liquids. It shows that a variety of these fillers are commonly employed alongside ionic liquids to enhance the properties of polymer composites. Among these, multiwalled carbon nanotubes appear frequently, indicating their significant role and effectiveness in composite enhancements when modified by ionic liquids [13,30,31,33]. This is followed by graphene oxide, which also exhibits a high frequency of use, underscoring its versatility and favorable properties that benefit from ionic liquid modification [18,29,34]. Graphene, known for its exceptional thermal, electrical, and mechanical properties [15,35,36], similarly attracts attention in modifications. In the past 5 years, there has been a significant increase in the number of publications on carbon-based fillers modified with ionic liquids, particularly graphene and graphene oxide, compared to multiwalled carbon nanotubes, as shown in Figure 1 from the Scopus database. Scientific studies focusing on polymer composites and their analysis via Raman spectroscopy were considered for inclusion in the data figure. Besides that, the usage of reduced graphene oxide also highlights its importance in specific applications where its distinct properties are advantageous. Carbon black, carboxylated multiwalled carbon nanotubes, and rice bran carbon, while less frequently mentioned, are indicative of the ongoing exploration into diverse carbon structures that can be potentially enhanced by ionic liquids for specialized applications. Generally, the usage frequency of these carbon-based fillers reflects the expanding interest and continuous innovation in the field of materials science, particularly in tailoring the interfacial interactions

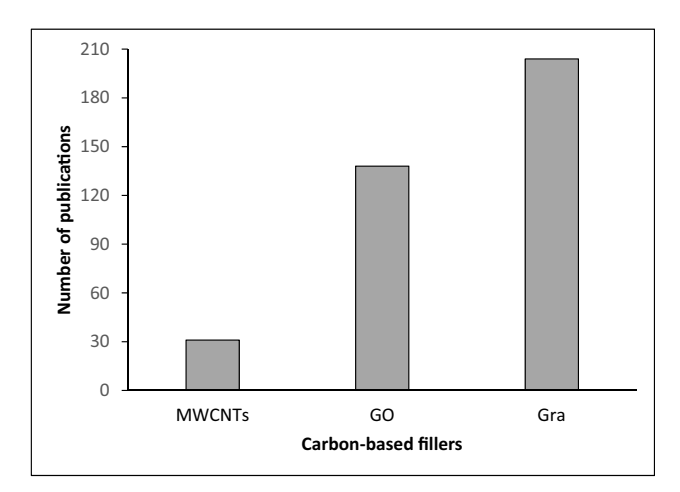


Figure 1: Number of publications on carbon-based fillers modified with ionic liquids, sourced from the Scopus database.

and performance features of polymer composites through advanced chemical modifications.

3 Ionic liquids for modification of carbon-based fillers

Table 2 shows examples of ionic liquids utilized in the modification of carbon-based fillers. It reflects a broad range of chemical structures tuned for specific interactions with carbon materials in polymer composites. Among these, 1-butyl-3methylimidazolium hexafluorophosphate (BmimPF₆) seems to stand out for its frequent use, highlighting its efficacy and versatility in modifying fillers to improve composite properties such as conductivity and mechanical strength [35,38,42,47]. Similarly, 1-butyl-3-methylimidazolium tetrafluoroborate (BmimBF₄) also shows significant utilization, suggesting its suitability in achieving desired dispersion and interfacial adhesion within composites [13,15,38]. The utilization of 1-ethyl-3-methylimidazolium tetrafluoroborate (EmimBF₄) also illustrates the expansive approach researchers take to optimize the interaction between fillers and polymer matrices [3,27,48]. There has been a substantial rise in the number of publications on ionic liquids utilized for modifying carbon-based fillers in the past 5 years, specifically BmimBF₄ compared to BmimPF₆, as shown in Figure 2 from the Scopus database. In addition, this review applied the Scopus database as it offers a more significant number of publications than the Web of Science database [52,53]. Figure 3 shows the chemical structures of BmimPF₆, BmimBF₄, and EmimBF₄. The specific choices of these ionic liquids are driven by their ability to tune the surface properties of carbon-based fillers, enhancing compatibility with polymers and overall material performance. Moreover, less common but specialized ionic liquids indicate ongoing explorations into new chemistry. In general, the selection and frequency of these ionic liquids in modifications denote a strategic approach to improving the performance characteristics of carbon-based filler composites, with a continuous push towards more innovative and effective material solutions.

4 Polymer matrices for ionic liquidmodified carbon-based filler/ polymer composites

Table 3 displays examples of polymer matrices employed in ionic liquid-modified carbon-based filler/polymer composites. Among these, styrene-butadiene rubber (SBR) is

Table 2: Examples of ionic liquids utilized in the modification of carbon-based fillers

Ionic liquid	Abbreviation	Ref.
1-Allyl-3-methylimidazolium chloride	AmimCl	[9,45]
3-Allyl-1-methylimidazolium hexafluorophosphate	AmimPF ₆	[27,48]
1-(2-Aminoethyl)-3-methylimidazolium bromide	AemimBr	[23]
1-(3-Aminopropyl)-3-butylimidazolium bis(trifluoromethylsulfonyl)imide	ApbimTFSI	[6]
1-(3-Aminopropyl)-3-butylimidazolium bromide	ApbimBr	[6]
1-Benzyl-3-methylimidazolium chloride	BzmimCl	[25,31,49]
1-Benzyl-3-methylimidazolium tetrafluoroborate	$BzmimBF_4$	[19]
1-(3-Butoxy-2-hydroxypropyl)-3-methylimidazolium tetrafluoroborate	$BhpmimBF_4$	[18]
1-Butyl-3-methylimidazolium bis(trifluoromethylsulfonyl)imide	BmimTFSI	[28,46]
1-Butyl-3-methylimidazolium hexafluorophosphate	BmimPF ₆	[27,35,38,42,47,48]
1-Butyl-3-methylimidazolium tetrafluoroborate	BmimBF ₄	[13,15,17,38]
1-Butyl-1-methylpyrrolidinium hexafluorophosphate	BmpyPF ₆	[40]
1-Butylpyridinium bromide	BpyBr	[39]
1-Carboxyethyl-3-methylimidazolium bis(trifluoromethylsulfonyl)imide	CemimTFSI	[37]
1-Decyl-3-methylimidazolium chloride	DmimCl	[33]
1-Ethyl-2,3-dimethylimidazolium bis(trifluoromethylsulfonyl)imide	EdmimTFSI	[7]
1-Ethyl-3-methylimidazolium bis(trifluoromethylsulfonyl)imide	EmimTFSI	[34]
1-Ethyl-3-methylimidazolium bromide	EmimBr	[43]
1-Ethyl-3-methylimidazolium dicyanamide	EmimDCA	[14,50]
1-Ethyl-3-methylimidazolium tetrafluoroborate	EmimBF ₄	[3,27,48]
1-Hexyl-3-methylimidazolium bromide	HmimBr	[43]
1-Hexyl-3-methylimidazolium hexafluorophosphate	HmimPF ₆	[51]
1-Hydroxyethyl-3-methylimidazolium tetrafluoroborate	HemimBF ₄	[24]
4-Methyl-1-butylpyridinium bromide	MbpyBr	[39]
1-Methylimidazolium chloride	MimCl	[29]
1-Methyl-3-octylimidazolium chloride	MoimCl	[45]
1-Methyl-3-pyrenylmethylimidazolium hexafluorophosphate	MpmimPF ₆	[35]
3,3'-(Octane-1,8-diyl)bis(1-butyl-imidazolium) bromide	OdbbimBr	[22]
1-Octyl-3-methylimidazolium tetrafluoroborate	OmimBF ₄	[11,26]
Tributylmethylammonium bis(trifluoromethylsulfonyl)imide	TbmamTFSI	[3]
Trihexyl(tetradecyl)phosphonium bistriflimide	ThtdphTFSI	[30]
Trihexyl(tetradecyl)phosphonium bis(2,4,4-trimethylpentyl)phosphinate	ThtdphTMPP	[2]
1-Vinyl-3-ethylimidazolium bromide	VeimBr	[44]
1-Vinyl-3-ethylimidazolium tetrafluoroborate	VeimBF ₄	[16,20,41]
1-Vinyl-3-hexylimidazolium bromide	VhimBr	[44]

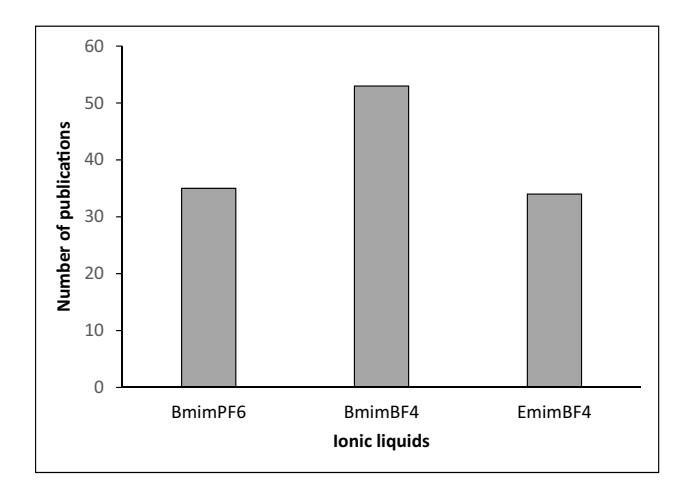


Figure 2: Number of publications on ionic liquids utilized for modifying carbon-based fillers, sourced from the Scopus database.

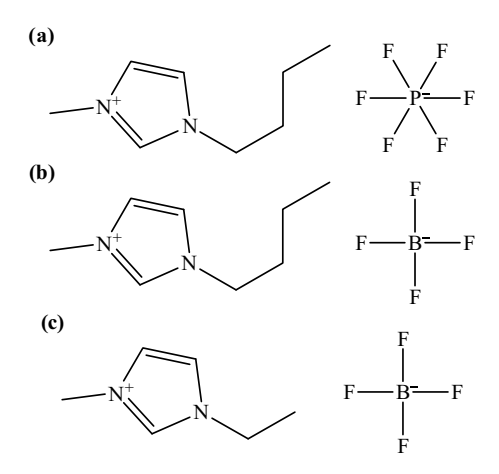


Figure 3: Chemical structures of (a) $BmimPF_6$, (b) $BmimBF_4$, and (c) $EmimBF_4$.

Table 3: Examples of polymer matrices employed in ionic liquid-modified carbon-based filler/polymer composites

Polymer matrix	Abbreviation	Ref.
Bromobutyl rubber	BIIR	[42]
Carboxylated nitrile rubber	XNBR	[34]
Carboxylated SBR	XSBR	[51]
Diglycidyl ester of aliphatic	DGEAC	[18]
cyclo		
Diglycidyl ether of bisphenol A	DGEBA	[2,13,22]
Ethylene acrylic elastomer	AEM	[45]
Ethylene–vinyl acetate	EVM	[3]
copolymer		
Fluorinated elastomer	FKM	[50]
High amorphous polyvinyl	HAVOH	[49]
alcohol		
Natural rubber latex	NRL	[43]
Nitrile butadiene rubber	NBR	[24]
Poly(ε-caprolactone)	PCL	[48]
Polychloroprene rubber	CR	[28,37]
Polyetherimide	PEI	[17,35,47]
Polyimide	PI	[15]
Polylactic acid	PLA	[40]
Polymethylmethacrylate	PMMA	[11,26]
Polystyrene	PS	[30]
Polyurethane	PU	[29]
Polyvinyl chloride	PVC	[19]
Polyvinylidene fluoride	PVDF	[16,20,23,27,38,41]
Silicone rubber	QM	[14]
Sodium polyacrylate	PAA	[6]
Styrene-butadiene rubber	SBR	[7,9,25,31,33,39,46]
Thermoplastic polyurethane	TPU	[44]

particularly prominent, highlighting its significance in improving the toughness and abrasion resistance of composites [39], which are crucial attributes in automotive and industrial applications. Polyvinylidene fluoride (PVDF) also has significant features, indicating its widespread acceptance and effectiveness in achieving desired mechanical, thermal, and electrical properties in composites. This polymer is favored due to its excellent chemical resistance and piezoelectric properties [23,27], which are beneficial in various applications, including sensors and actuators. Another polymer, like polyetherimide (PEI), appears less frequently but is important for specific properties it imparts, such as high-temperature resistance [17]. Similarly, diglycidyl ether of bisphenol A (DGEBA), commonly used in epoxy resins, is noted for its strong mechanical strength and chemical resistance, making it a preferred choice for high-performance applications [22]. Figure 4 shows the chemical structures of SBR, PVDF, PEI, and DGEBA. The variety of polymers listed, ranging from elastomers to advanced engineering plastics, reflects the broad applicability and customization potential of carbon-based polymer composites modified by ionic liquids.

This diverse array of polymer matrices employed suggests ongoing efforts to meet specific performance criteria across various industries, driving forward innovations in composite material technologies.

5 Raman spectroscopy analysis of ionic liquid-modified carbonbased fillers and their polymer composites

Raman spectroscopy serves as a necessary instrument in the analysis of ionic liquid-modified carbon-based fillers and their polymer composites, offering crucial insights through the observation of two significant characteristic peaks such as the D (diamondoid) peak [34] and G (graphitic) peak [29,54] in the Raman spectra. Figure 5 displays the Raman spectrum of graphene oxide, an example of carbon-based fillers. The D peak is mainly located around 1,200 and 1,499 cm⁻¹, indicative of defects or disorders within the carbon structures [25], and the G peak is situated chiefly around 1,400 and 1,699 cm⁻¹, representative of the graphitic domain [23]. These peaks are pivotal in assessing the modifications introduced by ionic liquids. Modifications with ionic liquids can result in observable shifts in these peak positions. The shifts in D and G peak positions often imply chemical interactions between the ionic liquids and the carbon-based fillers [3,43] and between the ionic liquid-modified carbon-based fillers and the polymer matrices [17,31,45]. Furthermore, the intensity ratios between these peaks $(I_D/I_G$ ratio) provide additional data points [55]. The intensity ratios typically signify structural defects/disorders [35] or the crystallinity of carbon materials [48]. Through these detailed analyses, Raman spectroscopy elucidates the molecular-level interactions and structural rearrangements occurring in modified carbon-based fillers and their composites, making it an essential method for advancing the development of high-performance materials with tailored properties.

5.1 Raman analysis of ionic liquid-modified carbon-based fillers

Table 4 exhibits the Raman peaks, peak positions, and intensity ratios of various carbon-based fillers modified with different ionic liquids acquired using different equipment and laser wavelengths. A significant observation from the table is the prevalence of upshifted peak positions

$$(a)$$

$$(b)$$

$$F$$

$$n$$

$$(e)$$

$$(d)$$

$$(d)$$

$$(d)$$

$$(d)$$

$$(d)$$

$$(d)$$

$$(d)$$

$$(e)$$

$$(d)$$

$$(e)$$

$$(e)$$

$$(e)$$

$$(f)$$

$$(f$$

Figure 4: Chemical structures of (a) SBR, (b) PVDF, (c) PEI, and (d) DGEBA.

in many combinations, particularly with MWCNTs. This suggests that the interaction between this filler and certain ionic liquids, such as imidazolium-based ionic liquids with hexafluorophosphate, bis(trifluoromethylsulfonyl)imide, tetrafluoroborate, and bromide counter anions. This leads to considerable interaction with the π -electronic nanotube network or surface [7,43], which is detectable via Raman spectroscopy. Besides that, GO displays a variety of peak positions with different ionic liquids, indicating a versatile response to modifications, which could be attributed to its unique oxygen-containing functional groups that interact variably with different ionic liquids [11,18,23]. Upshifted peak positions are notably common with ionic liquids like AemimBr, EmimTFSI, and OmimBF4, implying enhanced interactions that might influence their properties [26,34]. Generally, the table indicates that the type of ionic liquid

profoundly affects the Raman spectra results of carbon-based fillers, suggesting modifications that can be crucial for tuning the properties of carbon materials for specific applications. The ability of certain ionic liquids to consistently induce upshifted peak positions in MWCNTs and GO underscores their potential for enhancing material characteristics in advanced composites.

Another observation from Table 4 is the higher intensity ratio seen in most combinations, indicating reduced ordering or decreased crystallinity, which could translate to the formation of amorphous carbon at the molecular level [26,29,34]. This formation typically indicates the effective surface modification of carbon-based fillers by the ionic liquid molecules [18,27]. GO consistently shows higher intensity ratios with various ionic liquids. This consistency across different ionic liquids implies that GO is particularly

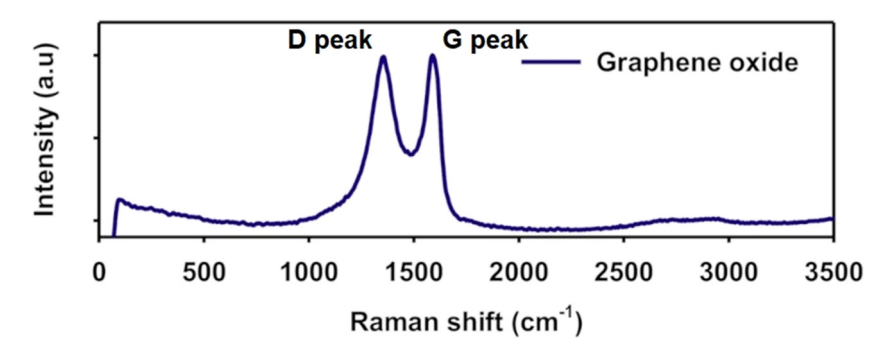


Figure 5: Raman spectrum of graphene oxide. Reproduced from Sánchez-Rodríguez et al. [40].

Table 4: Raman peaks, peak positions, and intensity ratios of ionic liquid-modified carbon-based fillers acquired using different equipment and laser wavelengths

Carbon-based filler	Ionic liquid	Raman peak (cm ⁻¹)	Peak position	Intensity ratio	Equipment	Laser wavelength (nm)	Ref.
СВ	VeimBF ₄	Unstated	Unstated	High	B, Senterra R200	785	[16]
Gra	BmimBF ₄	1,581	Downshift	High	TS, DXR	532	[15]
Gra	BmimPF ₆	1,349, 1,581	Upshift	Low	R, inVia Reflex	532	[35]
Gra	HemimBF ₄	1,344, 1,580	Downshift	Unstated	Unstated	Unstated	[24]
Gra	OdbbimBr	1,340, 1,581	Downshift	Low	R, inVia Reflex	Unstated	[22]
GO	AemimBr	1,352, 1,591	Upshift	High	Unstated	Unstated	[23]
GO	AmimCl	1,342, 1,579	Downshift	High	R, inVia-H31894	514.5	[9]
GO	BhpmimBF ₄	Unstated	Downshift	High	TY-HR 800	514	[18]
GO	BmimPF ₆	1,345, 1,590	Downshift	High	R, inVia-H31894	514.5	[42]
GO	EmimDCA	1,353, 1,586	Unchanged	High	Unstated	Unstated	[14]
GO	EmimTFSI	1,353, 1,592	Upshift	High	H, Jobin Yvon T64000	514.5	[34]
GO	OmimBF ₄	1,345, 1,583	Upshift	High	W, Access 300	532	[26]
GO	OmimBF ₄	1,357, 1,594	Unchanged	High	R, inVia	514	[11]
GO	MimCl	Unstated	Unstated	High	Unstated	Unstated	[29]
GO	VeimBF ₄	1,260	Downshift	High	B, Senterra, R200	785	[41]
RGO	BzmimBF ₄	1,334, 1,586	Upshift	Unstated	W, alpha 300RA	633	[19]
RGO	EmimDCA	1,332, 1,573	Downshift	High	W, alpha 300RA	Unstated	[50]
MWCNTs	ApbimTFSI	1,346, 1,583	Upshift	High	R, inVia Qontor	514	[6]
MWCNTs	BmimBF₄	1,345, 1,575	Unchanged	High	R, inVia	514	[13]
MWCNTs	BmimBF ₄	1,346, 1,588	Upshift	Unstated	R, inVia Reflex	532	[17]
MWCNTs	BmimPF ₆	1,311, 1,589	Upshift	Unstated	H, ARAMIS UV	785	[47]
MWCNTs	BmimPF ₆	1,356, 1,582	Upshift	High	R, inVia	514	[27]
MWCNTs	BmimPF ₆	1,359, 1,587	Upshift	High	R, inVia	514	[48]
MWCNTs	BmimTFSI	1,309, 1,605	Upshift	Low	Holoprobe 785	785	[28]
MWCNTs	DmimCl	1,351, 1,548	Downshift	High	W, alpha 300R	532	[33]
MWCNTs	EdmimTFSI	1,328, 1,571	Upshift	Low	Unstated	Unstated	[7]
MWCNTs	EmimBF ₄	1,309, 1,590	Upshift	Unstated	B, Senterra	785	[3]
MWCNTs	HmimBr	1,353, 1,589	Upshift	High	R, inVia Reflex	532	[43]
MWCNTs	ThtdphTFSI	1,345, 1,575	Unchanged	High	R, inVia	514	[30]
MWCNTs	ThtdphTMPP	1,345, 1,575	Unchanged	High	R, inVia	514	[2]
MWCNTs	VeimBF ₄	Unstated	Upshift	High	B, Senterra R200	785	[20]
MWCNTs	VhimBr	1,360, 1,580	Upshift	High	H, LabRam HR Evolution	532	[44]
MWCNT-COOH	CemimTFSI	1,349, 1,579	Upshift	Unstated	TS, DXR	532	[37]
RBC	HmimPF ₆	1,418, 1,598	Upshift	Unstated	B, Senterra R200-L	532	[51]

B = Bruker, H = Horiba, R = Renishaw, TS = Thermo Scientific, W = WiTec.

receptive to ionic liquid modification, potentially due to its oxygenated surface, which can facilitate diverse chemical interactions [14,23]. For MWCNTs, the higher intensity ratio is common, although there are exceptions with certain ionic liquids like BmimTFSI and EdmimTFSI showing a lower intensity ratio, certainly reflecting the rearrangement of the tubes or high degree of crystallinity that enhanced structural order to some extent [7,28]. In contrast, Gra exhibits both higher and lower intensity ratios depending on the specific ionic liquid used. In general, the table suggests that ionic liquids have a significant impact on the Raman spectra outcomes of these fillers, providing evidence of their potential to modify and feasibly improve the properties of carbon-based materials for polymer composites. This influence is crucial for designing materials tuned for specific applications where enhanced properties are required.

5.2 Raman analysis of ionic liquid-modified carbon-based filler/polymer composites

Table 5 demonstrates the Raman peaks, peak positions, and intensity ratios of diverse ionic liquid-modified carbonbased filler/polymer composites acquired using different 8 — Ahmad Adlie Shamsuri *et al.* DE GRUYTER

Table 5: Raman peaks, peak positions, and intensity ratios of ionic liquid-modified carbon-based filler/polymer composites acquired using different
equipment and laser wavelengths

Polymer composite	Ionic liquid	Raman peak (cm ⁻¹)	Peak position	Intensity ratio	Equipment	Laser wavelength (nm)	Ref.
AEM/MWCNTs	MoimCl	1,610	Upshift	Unstated	Unstated	Unstated	[45]
DGEAC/GO	BhpmimBF ₄	1,335	Upshift	Unstated	TY-HR 800	514	[18]
HAVOH/MWCNTs	BzmimCl	1,355, 1,598	Upshift	Low	W, UHTS 300	532	[49]
PCL/MWCNTs	BmimPF ₆	1,360, 1,588	Upshift	High	R, inVia	514	[48]
PEI/MWCNTs	BmimBF ₄	Unstated	Upshift	Unstated	R, inVia Reflex	532	[17]
PMMA/GO	OmimBF ₄	1,356, 1,588	Upshift	High	W, Access 300	532	[26]
PVDF/Gra	BmimPF ₆	Unstated	Unstated	High	J, NRS-5100	532	[38]
PVDF/GO	VeimBF ₄	1,320	Downshift	High	B, Senterra, R200	785	[41]
PVDF/MWCNTs	BmimPF ₆	1,353, 1,583	Upshift	High	R, inVia	514	[27]
PVDF/MWCNTs	VeimBF ₄	Unstated	Upshift	High	B, Senterra R200	785	[20]
QM/GO	EmimDCA	1,260, 1,410	Downshift	Low	Unstated	Unstated	[14]
SBR/MWCNTs	BzmimCl	Unstated	Downshift	Low	Unstated	Unstated	[31]

B = Bruker, J = JASCO, R = Renishaw, W = WiTec.

equipment and laser wavelengths. A Raman analysis of the AEM/MWCNTs-MoimCl composites was conducted by Prasad Sahoo *et al.* [45]. Figure 6 shows the Raman spectra of the composites (a) and pristine MWCNTs (b). They found that the G peak position of the composites upshifted to 1,610 cm⁻¹, compared to 1,589 cm⁻¹ for pristine MWCNTs. This upshift is associated with the untangling of the MWCNTs and their subsequent distribution within the AEM matrix. The untangling of the MWCNTs results from robust chemical interactions between the AEM matrix and MWCNTs-MoimCl [45].

A Raman analysis of the DGEAC/GO-BhpmimBF₄ composites was carried out by Shi *et al.* [18]. They discovered that the D peak position of the composites upshifted to 1,335 cm⁻¹, compared to 1,330 cm⁻¹ for the DGEAC/GO composite. This upshift, which may be caused by changes in atomic distances due to the presence of BhpmimBF₄ in the composites, is definitely correlated with the degree of deformation [18].

A Raman analysis of the HAVOH/MWCNTs-BzmimCl composites was conducted by Santillo *et al.* [49]. Figure 7 displays the Raman spectra of the composites (a) and pristine MWCNTs

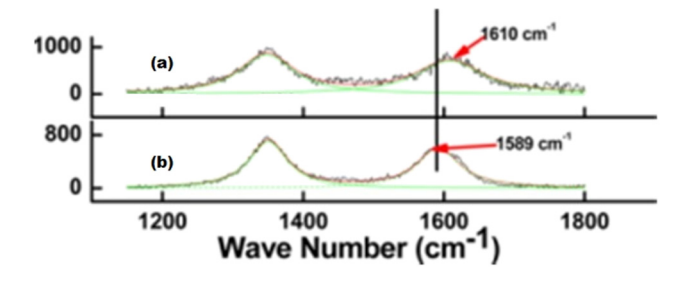


Figure 6: Raman spectra of AEM/MWCNTs-MoimCl composites (a) and pristine MWCNTs (b). Reproduced from Prasad Sahoo *et al.* [45], with permission from John Wiley and Sons.

(b). They found that the D and G peak positions of the composites upshifted to 1,355 and 1,598 cm⁻¹, respectively, compared to 1,348 and 1,591 cm⁻¹ for pristine MWCNTs. This upshift is due to BzmimCl, which contains imidazolium and benzyl groups and forms π – π interactions with MWCNTs, as well as hydrogen bonding with HAVOH [49]. However, the intensity ratio of the composites is lower than that of pristine MWCNTs. This lowered intensity ratio indicates reduced shear stress among MWCNTs and fewer structural defects [49].

A Raman analysis of the PCL/MWCNTs-BmimPF $_6$ composites was carried out by Yoon *et al.* [48]. Figure 8 shows the Raman spectra of the composites (a) and pure MWCNTs

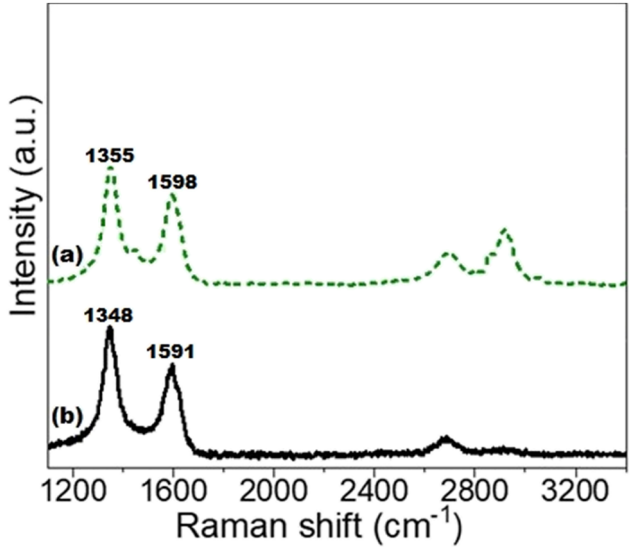


Figure 7: Raman spectra of HAVOH/MWCNTs-BzmimCl composites (a) and pristine MWCNTs (b). Reproduced from Santillo *et al.* [49], with permission from Elsevier.

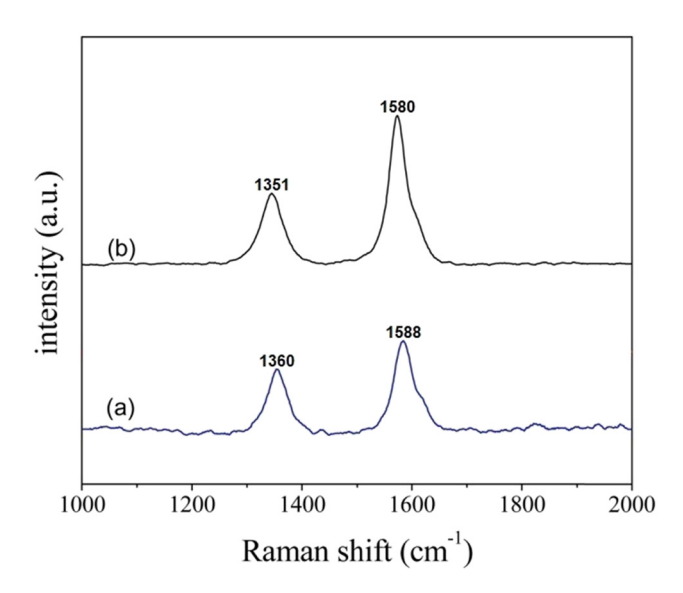


Figure 8: Raman spectra of PCL/MWCNTs-BmimPF₆ composites (a) and pure MWCNTs (b). Reproduced from Yoon *et al.* [48], with permission from John Wiley and Sons.

(b). They discovered that the D and G peak positions of the composites upshifted to 1,360 and 1,588 cm $^{-1}$, respectively, compared to 1,351 and 1,580 cm $^{-1}$ for pure MWCNTs. This upshift is attributed to the strong interaction between BmimPF $_6$ and MWCNTs in the PCL matrix [48]. Moreover, the intensity ratio of the composites is higher than that of pure MWCNTs. This higher intensity ratio suggests that the inclusion of BmimPF $_6$ introduces additional defects in the MWCNTs [48].

A Raman analysis of the PEI/MWCNTs-BmimBF $_4$ composites was conducted by Ke *et al.* [17]. Figure 9 displays the

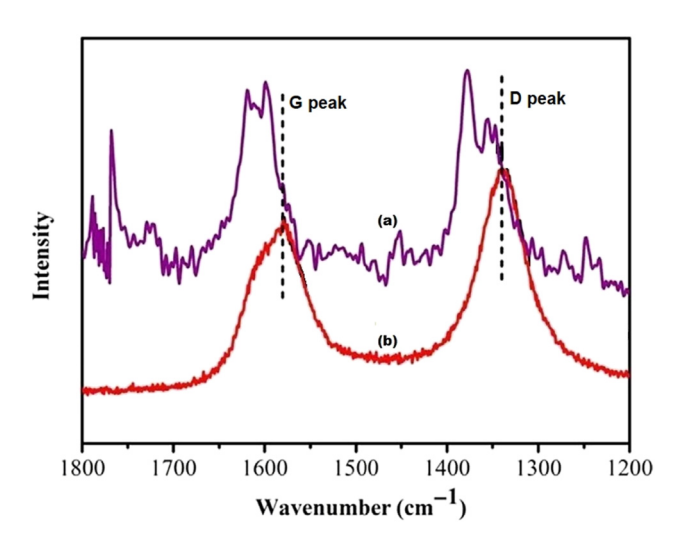


Figure 9: Raman spectra of PEI/MWCNTs-BmimBF $_4$ composites (a) and pristine MWCNTs (b). Reproduced from Ke *et al.* [17], with permission from John Wiley and Sons.

Raman spectra of the composites (a) and pristine MWCNTs (b). They found that the D and G peak positions of the composites upshifted relative to those of pristine MWCNTs. This substantial upshift indicates that the MWCNTs-BmimBF₄ are encapsulated within the PEI matrix, indicating a strong interaction between the two components [17].

A Raman analysis of the PMMA/GO-OmimBF₄ composites was carried out by Minguez-Enkovaara *et al.* [26]. They discovered that the D and G peak positions of the composites upshifted to 1,356 and 1,588 cm⁻¹, respectively, compared to 1,355 and 1,580 cm⁻¹ for pristine GO. This upshift is induced by the presence of OmimBF₄. Moreover, the intensity ratio of the composites is higher than that of pristine GO. This higher intensity ratio is due to the reduced crystallite size of GO-OmimBF₄ within the PMMA matrix [26].

A Raman analysis of the PVDF/Gra-BmimPF $_6$ composites was conducted by Widakdo *et al.* [38]. They found that the intensity ratio of the composites increased with the BmimPF $_6$ content. The increase in intensity ratio is linked to a marked increase in disorder within the Gra structure. This defect is likely caused by bulky Bmim cations on the surface, which introduce a degree of strain [38].

A Raman analysis of the PVDF/GO-VeimBF₄ composites was carried out by Guan *et al.* [41]. Figure 10 shows the Raman spectra of the composites (a) and raw GO (b). They discovered that the D peak position of the composites downshifted to 1,320 cm⁻¹, compared to 1,333 cm⁻¹ for raw GO. This downshift is due to some grafted VeimBF₄ molecules being peeled off from the surface of GO [41]. However, the intensity ratio of the composites is higher than that of raw GO. This higher intensity ratio implies that the microphase-separated nanoclusters on the GO surface continue to interact with the GO surface [41].

A Raman analysis of the PVDF/MWCNTs-BmimPF $_6$ composites was conducted by Chen $\it et~al.~$ [27]. Figure 11 displays

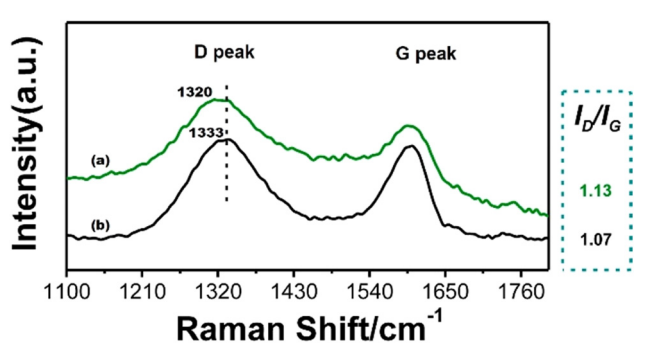


Figure 10: Raman spectra of PVDF/GO-VeimBF₄ composites (a) and raw GO (b). Reproduced from Guan *et al.* [41], with permission from Elsevier.

10 — Ahmad Adlie Shamsuri et al. DE GRUYTER

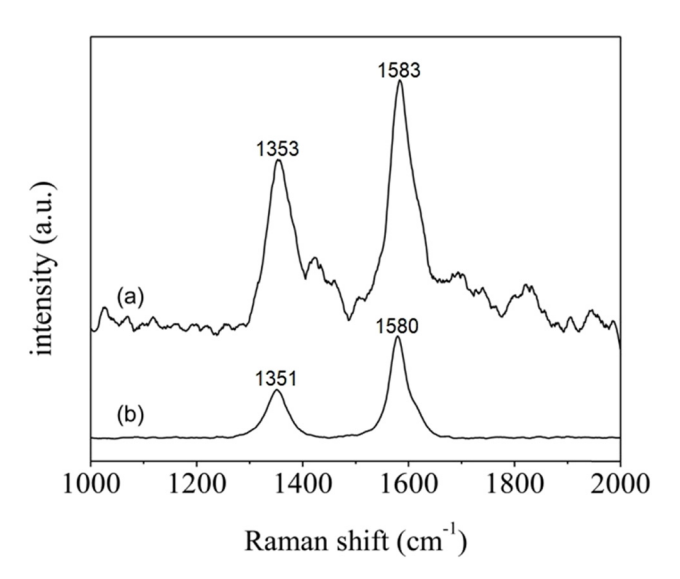


Figure 11: Raman spectra of PVDF/MWCNTs-BmimPF₆ composites (a) and pure MWCNTs (b). Reproduced from Chen *et al.* [27], with permission from John Wiley and Sons.

the Raman spectra of the composites (a) and pure MWCNTs (b). They found that the D and G peak positions of the composites upshifted to 1,353 and 1,583 cm $^{-1}$, respectively, compared to 1,351 and 1,580 cm $^{-1}$ for pure MWCNTs. This upshift is induced by the strong interaction between BmimPF $_6$ and MWCNTs in the PVDF matrix [27]. Moreover, the intensity ratio of the composites is higher than that of pure MWCNTs. This higher intensity ratio indicates that the introduction of BmimPF $_6$ into the composites can induce more defects in the MWCNTs [27].

A Raman analysis of the PVDF/MWCNTs-VeimBF $_4$ composites was carried out by Wang *et al.* [20]. Figure 12 shows the Raman spectra of the composites (a) and pristine MWCNTs (b). They discovered that the G peak position of the composites upshifted relative to that of pristine MWCNTs. This upshift is

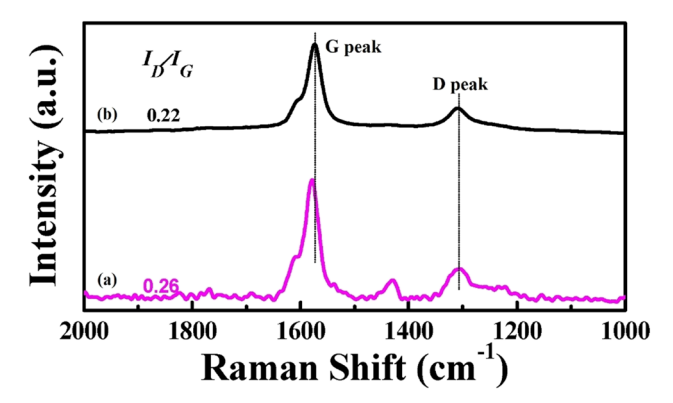


Figure 12: Raman spectra of PVDF/MWCNTs-VeimBF $_4$ composites (a) and pristine MWCNTs (b). Reproduced from Wang *et al.* [20].

attributed to the interactions between the cations of MWCNTs-VeimBF $_4$ and CF $_2$ groups in the PVDF matrix [20]. Furthermore, the intensity ratio of the composites is higher than that of pristine MWCNTs. This higher intensity ratio exhibits the detachment of VeimBF $_4$ from the MWCNTs [20].

A Raman analysis of the QM/GO-EmimDCA composites was conducted by Sarath *et al.* [14]. They found that the D and G peak positions of the composites downshifted to 1,260 and 1,410 cm⁻¹, respectively, compared to 1,353 and 1,586 cm⁻¹ for neat GO. This downshift is due to the interaction of GO-EmimDCA and QM matrix. Moreover, the intensity ratio of the composites is lower than that of neat GO. This lowered intensity ratio suggests fewer structural defects and edge effects associated with the narrow width of graphene sheets [14].

A Raman analysis of the SBR/MWCNTs-BzmimCl composites was carried out by Abraham *et al.* [31]. They discovered that the G peak position of the composites downshifted relative to that of pristine MWCNTs. This downshift is induced by the mechanical compression transferred from the SBR matrix to the MWCNTs, causing the MWCNTs-BzmimCl to shrink [31]. Furthermore, the intensity ratio of the composites is lower than that of pristine MWCNTs. This lowered intensity ratio results from improved alignment of MWCNTs within the composites and a decrease in disorder or the number of defects [31].

6 Discussion

Table 4 reveals changes in Raman peak positions and intensity ratios, illustrating the complex interactions between various carbon-based fillers and ionic liquids. MWCNTs often show upshifted peak positions, likely due to significant interactions with ionic liquids like imidazolium-based ionic liquids. These interactions with the nanotube's π -electronic network are detectable via Raman spectroscopy and suggest a strong interaction that modifies the electronic structure of the carbon nanotubes. Conversely, GO displays varied responses to ionic liquid modifications, possibly because its oxygen-containing functional groups interact differently with various ionic liquids. The consistent upshift in GO's peak positions with certain ionic liquids indicates enhanced interactions that can significantly influence its properties, indicating the potential for tailored functionalization. Moreover, a higher intensity ratio across most modified carbon fillers implies a decrease in crystallinity or ordering, often translating to increased amorphous carbon content. This is indicative of effective surface modification, especially noted in GO, which consistently shows this characteristic across

different ionic liquids, pointing to its high receptiveness to modification due to its oxygenated surface. For MWCNTs, variations in intensity ratios could reflect changes in structural ordering or crystallinity, highlighting the subtle effects of specific ionic liquids. Overall, these spectra changes underline the deep impact of ionic liquids on carbon fillers, enhancing their properties for use in advanced composites and underscoring their potential in material design customized for specific applications.

Table 5 showcases Raman spectra changes across various ionic liquid-modified carbon-based filler/polymer composites, reflecting involved interactions at the molecular level. Across different studies, a common observation is the upshift in both D and G peak positions in composites, indicating alterations in the electronic properties and structural rearrangements due to the interactions between the fillers and the ionic liquids. These upshifts, often linked to the redistribution of modified carbon fillers within the matrices, suggest robust chemical interactions that alter the properties of the composites. Similarly, downshifts in peak positions are typically associated with the detachment or reorganization of modified fillers, affecting their interaction with surrounding polymer matrices. This change of peak positions highlights the specific impacts of various ionic liquids, such as imidazolium-based ionic liquids with different counter anions, on the structural integrity and electronic characteristics of the fillers. The intensity ratios, another critical measure of Raman spectroscopy, provide insights into the degree of disorder or crystallinity within the composites. Higher intensity ratios generally indicate increased amorphous characteristics or structural defects. Conversely, lower intensity ratios suggest enhanced ordering, which can be a result of fewer structural defects or disorders. By analyzing these Raman spectra as a whole, it is evident that ionic liquids play a transformative role in tuning the properties of carbon-based materials, enhancing their utility in advanced polymer composites.

7 Conclusions

In this review, examples of carbon-based fillers used for modification, ionic liquids utilized in the modification, and polymer matrices employed in polymer composites are concisely identified. Additionally, the interactional and structural properties of carbon-based fillers and their polymer composites, as analyzed by Raman spectroscopy, are described in this concise review. MWCNTs, GO, and Gra are the most commonly used carbon-based fillers for modification with ionic liquids, showcasing their critical role and efficiency in

enhancing polymer composites. BmimPF₆, BmimBF₄, and EmimBF₄ are the most frequently utilized ionic liquids in the modification of carbon-based fillers, reflecting their effectiveness and adaptability in improving the properties of polymer composites. SBR and PVDF are the most often employed polymer matrices in ionic liquid-modified carbonbased filler/polymer composites, emphasizing their importance in boosting the toughness and chemical resistance of these materials. Many Raman analyses show that carbonbased fillers modified with ionic liquids exhibit upshifted peak positions and higher intensity ratios compared to pristine carbon-based fillers. The upshifted peak positions suggest interactions between the fillers and ionic liquids, while the higher intensity ratios indicate structural defects in the modified fillers. Similarly, ionic liquid-modified carbon-based filler/polymer composites display upshifted peak positions and higher intensity ratios than their unmodified fillers. These upshifts are attributed to strong interactions between the modified fillers and polymer matrices, whereas the higher intensity ratios result from increased structural disorders in the modified fillers within the polymer matrices.

Acknowledgments: The authors appreciate the editors and reviewers for their valuable and supportive feedback throughout the review process.

Funding information: This concise review was supported by the Universiti Putra Malaysia under the Grant Putra IPM Scheme (project number: GP-IPM/2024/9789200).

Author contributions: Ahmad Adlie Shamsuri: conceptualization, funding acquisition, investigation, project administration, and writing - original draft preparation; Mohd Zuhri Mohamed Yusoff: resources, supervision, and validation; Khalina Abdan: data curation and writing – review and editing; Siti Nurul Ain Md. Jamil: formal analysis and methodology. All authors have accepted responsibility for the entire content of this manuscript and approved its submission.

Conflict of interest: The authors state no conflict of interest.

References

- Shamsuri, A. A., S. N. A. Md. Jamil, M. Z. M. Yusoff, and K. Abdan. [1] Methods and mechanical properties of polymer hybrid composites and hybrid polymer composites: Influence of ionic liquid addition, Applied Mechanics, Vol. 5, No. 1, 2024, pp. 1-19.
- Soares, B. G., N. Riany, A. A. Silva, G. M. O. Barra, and S. Livi. Dualrole of phosphonium - Based ionic liquid in epoxy/MWCNT

- systems: Electric, rheological behavior and electromagnetic interference shielding effectiveness, *European Polymer Journal*, Vol. 84, 2016, pp. 77–88.
- [3] Cao, X., M. Jin, Y. Liang, and Y. Li. Synergistic effects of two types of ionic liquids on the dispersion of multiwalled carbon nanotubes in ethylene–vinyl acetate elastomer: preparation and characterization of flexible conductive composites, *Polymer International*, Vol. 66, No. 12, 2017, pp. 1708–1715.
- [4] Shamsuri, A. A., K. Abdan, M. Z. M. Yusoff, and S. N. A. M. Jamil. Impact of ionic liquids on the thermal properties of polymer composites, e-Polymers, Vol. 24, No. 1, 2024, id. 20240020.
- [5] Gouda, K., S. Bhowmik, and B. Das. A review on allotropes of carbon and natural filler-reinforced thermomechanical properties of upgraded epoxy hybrid composite, *Reviews on Advanced Materials Science*, Vol. 60, No. 1, 2021, pp. 237–275.
- [6] Yuan, X., H. Liu, H. Yu, W. Ding, Y. Li, and J. Wang. High-performance sodium polyacrylate nanocomposites developed by using ionic liquid covalently modified multiwalled carbon nanotubes, *Journal of Applied Polymer Science*, Vol. 137, No. 39, 2020, pp. 1–12.
- [7] Abraham, J. M. A., P L. Kailas, and N. Kalarikkal. Developing highly conducting and mechanically durable styrene butadiene rubber composites with tailored microstructural properties by a green approach using ionic liquid modi fi ed MWCNTs, RSC Advances, Vol. 6, 2016, pp. 32493–32504.
- [8] Shamsuri, A. A., K. Abdan, and S. N. A. Md. Jamil. Utilization of ionic liquids as compatibilizing agents for polymer blends – preparations and properties, *Polymer-Plastics Technology and Materials*, Vol. 62, No. 8, 2023, pp. 1008–1018.
- [9] Yin, B., X. Zhang, X. Zhang, J. Wang, and Y. Wen. Ionic liquid functionalized graphene oxide for enhancement of styrene-butadiene rubber nanocomposites, *Polymers for Advanced Technologies*, Vol. 28, 2017, pp. 293–302.
- [10] Shamsuri, A. A., M. Z. M. Yusoff, K. Abdan, and S. N. A. M. Jamil. Flammability properties of polymers and polymer composites combined with ionic liquids, *e-Polymers*, Vol. 23, No. 1, 2023, id. 20230060.
- [11] Sanes, J., G. Ojados, R. Pamies, and M. D. Bermúdez. PMMA nanocomposites with graphene oxide hybrid nanofillers, *Express Polymer Letters*, Vol. 13, No. 10, 2019, pp. 910–922.
- [12] Shamsuri, A. A., K. Abdan, and S. N. A. Md. Jamil. Preparations and Properties of Ionic Liquid-Assisted Electrospun Biodegradable Polymer Fibers, *Polymers*, Vol. 14, No. 12, 2022, id. 2308.
- [13] Lopes Pereira, E. C. and B. G. Soares. Conducting epoxy networks modified with non-covalently functionalized multi-walled carbon nanotube with imidazolium-based ionic liquid, *Journal of Applied Polymer Science*, Vol. 133, No. 38, 2016, pp. 1–9.
- [14] Sarath, P. S., D. Pahovnik, P. Utroša, O. CanOnder, J. T. Haponiuk, S. Thomas, et al. Study the characteristics of novel ionic liquid functionalized graphene oxide on the mechanical and thermal properties of silicone rubber nanocomposites, *Journal of Polymer Research*, Vol. 28, No. 11, 2021, pp. 1–11.
- [15] Ruan, H., Q. Zhang, W. Liao, Y. Li, X. Huang, X. Xu, et al. Enhancing tribological, mechanical, and thermal properties of polyimide composites by the synergistic effect between graphene and ionic liquid, *Materials and Design*, Vol. 189, 2020, id. 108527.
- [16] Xing, C., Y. Wang, X. Huang, Y. Li, and J. Li. Poly(vinylidene fluoride) nanocomposites with simultaneous organic nanodomains and inorganic nanoparticles, *Macromolecules*, Vol. 49, No. 3, 2016, pp. 1026–1035.

- [17] Ke, F., X. Yang, M. Zhang, Y. Chen, and H. Wang. Preparation and properties of polyetherimide fibers based on the synergistic effect of carbon nanotubes and ionic liquids, *Polymer Composites*, Vol. 44, No. 12, 2023, pp. 8917–8927.
- [18] Shi, K., J. Luo, X. Huan, S. Lin, X. Liu, X. Jia, et al. Ionic liquid-graphene oxide for strengthening microwave curing epoxy composites, ACS Applied Nano Materials, Vol. 3, No. 12, 2020, pp. 11955–11969.
- [19] Hafusa, A., M. R. G. Nair, N. Kalarickal, and S. Thomas. Impact of ionic liquid on the dielectric and mechanical performance of poly (Vinyl chloride) (PVC)/reduced graphene oxide (RGO) nanocomposites, *Macromolecular Symposia*, Vol. 398, No. 1, 2021, pp. 1–10.
- [20] Wang, Y. C., Xing J., Guan, and Y. Li. Towards flexible dielectric materials with high dielectric constant and low loss: PVDF nanocomposites with both homogenously dispersed CNTs and ionic liquids nanodomains, *Polymers*, Vol. 9, No. 11, 2017, id. 562.
- [21] Shamsuri, A. A., S. N. A. M. Jamil, and K. Abdan. The influence of ionic liquid pretreatment on the physicomechanical properties of polymer biocomposites: A mini-review, *e-Polymers*, Vol. 22, No. 1, 2022, pp. 809–820.
- [22] Sui, P. S., C. B. Liu A. M. Zhang, S. U. N. Cong, L. Y. Cui, and R. C. Zeng. Superior corrosion resistance and thermal/electro properties of graphene–epoxy composite coating on Mg alloy with biomimetic interface and orientation, *Transactions of Nonferrous Metals Society of China (English Edition)*, Vol. 34, 2024, pp. 157–170.
- [23] Maity, N., A. Mandal, and A. K. Nandi. Interface engineering of ionic liquid integrated graphene in poly(vinylidene fluoride) matrix yielding magnificent improvement in mechanical, electrical and dielectric properties, *Polymer*, Vol. 65, 2015, pp. 154–167.
- [24] Yang, X., Z. Zhang, T. Zhang, M. Nie, and Y. Li. Improved tribological and noise suppression performance of graphene/nitrile butadiene rubber composites via the exfoliation effect of ionic liquid on graphene, *Journal of Applied Polymer Science*, Vol. 137, No. 46, 2020, pp. 1–12.
- [25] Abraham, J., T. Jose, S. C. George, N. Kalarikkal, and S. Thomas. Mechanics and pervaporation performance of ionic liquid modified CNT Based SBR membranes - a case study for the separation of toluene/heptane mixtures, *International Journal of Membrane Science and Technology*, Vol. 2, 2015, pp. 30–38.
- [26] Minguez-Enkovaara, L. F., F. J. Carrión-Vilches, M. D. Avilés, and M. D. Bermúdez. Effect of graphene oxide and ionic liquid on the sliding wear and abrasion resistance of injection molded PMMA nanocomposites, *Express Polymer Letters*, Vol. 17, No. 3, 2023, pp. 237–251.
- [27] Chen, G., S. Zhang, Z. Zhou, and Q. Li. Dielectric properties of poly (vinylidene fluoride) composites based on Bucky gels of carbon nanotubes with ionic liquids, *Polymer Composites*, Vol. 36, No. 1, 2015, pp. 94–101.
- [28] Subramaniam, K., A. Das, D. Steinhauser, M. Klüppel, and G. Heinrich. Effect of ionic liquid on dielectric, mechanical and dynamic mechanical properties of multi-walled carbon nanotubes/ polychloroprene rubber composites, *European Polymer Journal*, Vol. 47, No. 12, 2011, pp. 2234–2243.
- [29] Mondal, T., S. Basak, and A. K. Bhowmick. Ionic liquid modification of graphene oxide and its role towards controlling the porosity, and mechanical robustness of polyurethane foam, *Polymer*, Vol. 127, 2017, pp. 106–118.
- [30] Soares da Silva, J. P., B. G. Soares, S. Livi, and G. M. O. Barra. Phosphonium-based ionic liquid as dispersing agent for MWCNT

- in melt-mixing polystyrene blends: Rheology, electrical properties and EMI shielding effectiveness, Materials Chemistry and Physics, Vol. 189, 2017, pp. 162-168.
- [31] Abraham, J., J. Thomas, N. Kalarikkal, S. C. George, and S. Thomas. Static and dynamic mechanical characteristics of ionic liquid modified MWCNT-SBR composites: theoretical perspectives for the nanoscale reinforcement mechanism, Journal of Physical Chemistry B, Vol. 122, No. 4, 2018, pp. 1525-1536.
- [32] Shamsuri, A. A., S. N. A. Md. Jamil, and K. Abdan. Coupling effect of ionic liquids on the mechanical, thermal, and chemical properties of polymer composites: A succinct review, Vietnam Journal of Chemistry, Vol. 62, No. 2, 2024, pp. 227-239.
- [33] Le, H. H., S. Wießner, A. Das, D. Fischer, M. Auf der Landwehr, Q. K. Do, et al. Selective wetting of carbon nanotubes in rubber compounds - Effect of the ionic liquid as dispersing and coupling agent, European Polymer Journal, Vol. 75, 2016, pp. 13-24.
- [34] Das, M., T. R. Aswathy, S. Pal, and K. Naskar. Effect of ionic liquid modified graphene oxide on mechanical and self-healing application of an ionic elastomer, European Polymer Journal, Vol. 158, 2021, id. 110691.
- [35] Wang, C., F. Ke, W. Fan, Y. Chen, F. Guan, S. Chen, et al. Efficient large-scale preparation of defect-free few-layer graphene using a conjugated ionic liquid as green media and its polyetherimide composite, Composites Science and Technology, Vol. 157, 2018, pp. 144-151.
- [36] Kośla, K., M. Olejnik, and K. Olszewska. Preparation and properties of composite materials containing graphene structures and their applicability in personal protective equipment: A Review, Reviews on Advanced Materials Science, Vol. 59, No. 1, 2020, pp. 215-242.
- [37] Jiang, G., S. Song, Y. Zhai, C. Feng, and Y. Zhang. Improving the filler dispersion of polychloroprene/carboxylated multi-walled carbon nanotubes composites by non-covalent functionalization of carboxylated ionic liquid, Composites Science and Technology, Vol. 123, 2016, pp. 171-178.
- [38] Widakdo, J., T.-J. Huang, T. M. Subrahmanya, H. F. M. Austria, H. L. Chou, W. S. Hung, et al. Bioinspired ionic liquid-graphene based smart membranes with electrical tunable channels for gas separation, Applied Materials Today, Vol. 27, 2022, id. 101441.
- [39] Gaca, M., M. Ilcikova, M. Mrlik, M. Cvek, C. Vaulot, P. Urbanek, et al. Impact of ionic liquids on the processing and photo-actuation behavior of SBR composites containing graphene nanoplatelets, Sensors and Actuators B: Chemical, Vol. 329, 2021, id. 129195.
- [40] Sánchez-Rodríguez, C., M. D. Avilés, R. Pamies, F. J. Carrión-vilches, J. Sanes, and M. D. Bermúdez. Extruded pla nanocomposites modified by graphene oxide and ionic liquid, Polymers, Vol. 13, No. 4, 2021, pp. 1-15.
- [41] Guan, J., C. Xing, Y. Wang, Y. Li, and J. Li. Poly (vinylidene fluoride) dielectric composites with both ionic nanoclusters and well dispersed graphene oxide, Composites Science and Technology, Vol. 138, 2017, pp. 98-105.
- [42] Xiong, X. J., Wang H., Jia E., Fang, and L. Ding. Structure, thermal conductivity, and thermal stability of bromobutyl rubber nanocomposites with ionic liquid modified graphene oxide, Polymer Degradation and Stability, Vol. 98, No. 11, 2013, pp. 2208-2214.

- [43] Ge, Y., Q. Zhang, Y. Zhang, F. Liu, and J. Han. High-performance natural rubber latex composites developed by a green approach using ionic liquid-modified multiwalled carbon nanotubes, Journal of Applied Polymer Science, Vol. 135, 2018, id. 46588.
- [44] Xu, Q. and W. Zhang. Improvement of the electromechanical properties of thermoplastic polyurethane composite by ionic liquid modified multiwall carbon nanotubes, E-Polymers, Vol. 21, No. 1, 2021, pp. 166-178.
- [45] Prasad Sahoo, B., K. Naskar, and D. Kumar. Tripathy. Multiwalled carbon nanotube-filled ethylene acrylic elastomer nanocomposites: Influence of ionic liquids on the mechanical, dynamic mechanical, and dielectric properties, Polymer Composites, Vol. 37, No. 8, 2016, pp. 2568-2580.
- [46] Subramaniam, K., A. Das, F. Simon, and G. Heinrich. Networking of ionic liquid modified CNTs in SSBR, European Polymer Journal, Vol. 49, No. 2, 2013, pp. 345-352.
- [47] Chen, Y., J. Tao, L. Deng, L. Li, J. Li, Y. Yang, et al. Polyetherimide/ bucky gels nanocomposites with superior conductivity and thermal stability, ACS Applied Materials and Interfaces, Vol. 5, No. 15, 2013, pp. 7478-7484.
- Yoon, S. W., X. Ren, and G. Chen. Preparation and dielectric properties of poly(ε-caprolactone) compounded with "bucky gels"-like mixture, Journal of Applied Polymer Science, Vol. 131, No. 10, 2014, id. 40231.
- Santillo, C., A. P. Godoy, R. K. Donato, R. J. E. Andrade, G. G. Buonocore, H. Xia, et al. Tuning the structural and functional properties of HAVOH-based composites via ionic liquid tailoring of MWCNTs distribution, Composites Science and Technology, Vol. 207, 2021, pp. 108742.
- [50] Moni, G., A. Mayeen, A. Mohan, J. J. George, S. Thomas, and S. C. George. Ionic liquid functionalised reduced graphene oxide fluoroelastomer nanocomposites with enhanced mechanical, dielectric and viscoelastic properties, European Polymer Journal, Vol. 109, 2018, pp. 277-287.
- Zhang, Y., X. Li, X. Ge, F. Deng, and U. R. Cho. Effect of coupling [51] agents and ionic liquid on the properties of rice bran carbon/carboxylated styrene butadiene rubber composites, Macromolecular Research, Vol. 23, No. 10, 2015, pp. 952-959.
- [52] Ahmad, W., H. Alabduljabbar, and A. F. Deifalla. An overview of the research trends on fiber-reinforced shotcrete for construction applications, Reviews on Advanced Materials Science, Vol. 62, No. 1, 2023, id. 20230144.
- [53] Khan, K. W., Ahmad M. N., Amin S. A., Khan A. F., Deifalla, and M. Y. M. Younes. Research evolution on self-healing asphalt: A scientometric review for knowledge mapping, Reviews on Advanced Materials Science, Vol. 62, No. 1, 2023, id. 20220331.
- [54] Alsaiari, N. S., M. S. Alsaiari, F. M. Alzahrani, A. Amari, and M. A. Tahoon. Synthesis, characterization, and application of the novel nanomagnet adsorbent for the removal of Cr(vi) ions, Reviews on Advanced Materials Science, Vol. 62, No. 1, 2023, id. 20230145.
- Ahmad, S. I., H. Hamoudi, A. Abdala, Z. K. Ghouri, and K. M. Youssef. [55] Graphene-reinforced bulk metal matrix composites: synthesis, microstructure, and properties, Reviews on Advanced Materials Science, Vol. 59, No. 1, 2020, pp. 67-114.